Taylor's regime of an autocatalytic reaction front in a pulsative periodic flow

M. Leconte, N. Jarrige, J. Martin, N. Rakotomalala, D. Salin, and L. Talon
Laboratoire Fluides, Automatique et Systèmes Thermiques, Universités P. et M. Curie and Paris Sud, C.N.R.S. (UMR 7608), Bâtiment 502, Campus Universitaire, 91405 Orsay Cedex, France

(Received 5 October 2007; accepted 1 April 2008; published online 27 May 2008)

Autocatalytic reaction fronts between reacted and unreacted species may propagate as solitary waves, that is, at a constant front velocity and with a stationary concentration profile, which result from a balance between molecular diffusion and chemical reaction. A velocity field in the supporting medium may affect the propagation of such fronts through different phenomena: advection, diffusion enhancement, front shape changes, etc. Here, we report on an experimental study and lattice Bhatnagar–Gross–Krook numerical simulations of the effect of an oscillating flow on the autocatalytic reaction between iodate and arsenous acid in a Hele–Shaw cell. In the low frequency range covered by the experiments, the front behavior is controlled by the flow across the gap and is reproduced with two-dimensional numerical simulations. It is shown that the front velocity oscillates at the frequency of the flow, whereas the front width oscillates at twice that frequency. Moreover, the Taylor regime in the presence of a Poiseuille flow is fully investigated: The description obtained in the case of a stationary flow provides an analytical prediction for the sinusoidal flow. The range of parameters, for which the prediction applies, is delineated and discussed. © *2008 American Institute of Physics*. [DOI: 10.1063/1.2919804]

INTRODUCTION

Interface motion and reaction front propagation occur in a number of different areas,[1] including flame propagation in combustion,[2] population dynamics,[3,4] and atmospheric chemistry (ozone hole). An autocatalytic reaction front between two reacting species propagates as a solitary wave, that is, at a constant front velocity and with a stationary front profile.[5,6] These issues were addressed earlier on, but only a few cases are understood, such as the pioneering works of Fisher[3] and Kolmogorov *et al.*[4] on a reaction-diffusion equation with a second-order kinetics.[1,7,8] Although the effect of an underlying flow on a flame propagation has been extensively analyzed,[2,7] the effect of advection on the behavior of an autocatalytic front has only recently been addressed.[9–12] In this case, the evolution of the concentration of each chemical species is given by the advection-diffusion-reaction (ADR) equation:

$$\frac{\partial C}{\partial t} + \vec{U} \cdot \vec{\nabla} C = D_m \Delta C + \alpha f(C), \tag{1}$$

where C is the normalized concentration of the (autocatalytic) reactant, $\vec{U}$ is the flow velocity, D_m is the molecular diffusion coefficient, and α is the reaction rate.

In the absence of flow ($\vec{U}=\vec{0}$), the balance between diffusion and reaction leads to a solitary wave of constant velocity V_χ and width l_χ. For the autocatalytic iodate-arsenous acid (IAA) reaction studied here, the kinetics is of the third order,[1] $f(C)=C^2(1-C)$, and the following one-dimensional solution of Eq. (1) is obtained:[1,6,13]

$$C(z,t) = \frac{1}{1+e^{(z-V_\chi t)/l_\chi}}, \quad l_\chi = \sqrt{\frac{2D_m}{\alpha}}, \quad V_\chi = \sqrt{\frac{\alpha D_m}{2}}, \tag{2}$$

where z is the direction of the front propagation. We note that propagating fronts with a stationary shape are also observed for quadratic reactions, such as the chlorite-tetrathionate reaction.[14,15] Thus, the present study, which is devoted to the IAA reaction, is expected to also apply to such higher order reactions.

For a reaction propagating along the direction of a unidirectional stationary flow $\vec{U}$, two regimes have been described, depending on the ratio $\phi=b/l_\chi$, where b is the typical length scale transverse to the flow direction.[16–18] In the eikonal regime, $\phi \gg 1$, the front propagates as a planar wave, at a velocity given by the sum of V_χ and of the algebraic maximum (along $\vec{V_\chi}$) of the flow velocity profile, and takes the according stationary form. In the mixing regime, $\phi \ll 1$, the interplay between diffusion and advection enhances the mixing of the chemical species and leads to an overall macroscopic diffusion known as the Taylor hydrodynamic dispersion.[19] The front propagation still obeys the same equation [Eq. (1)], in which the local fluid velocity and the molecular diffusion coefficient D_m have to be replaced by the transverse-averaged velocity and the effective macroscopic counterpart,[18] respectively. As a result, the front velocity is increased by either the mean advection velocity or the dispersion enhancement. The latter contribution, which brings the difference between the "classical" mixing regime, described in Ref. 16, and the Taylor regime, is usually negligible compared to the advection contribution. However, this Taylor regime has been tested and recovered, by numerical simulations, for the specific case of a stationary unidirec-

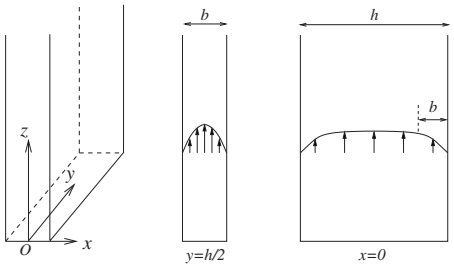

FIG. 1. Sketch of the HS cell of thickness b and width h. Also shown are the velocity profiles obtained at low frequency in the planes located at $y=h/2$ and at $x=0$.

tional flow with a sine velocity profile, namely, in the absence of mean advection. Note that for intermediate values of ϕ, an analytical fit of the front velocity has been recently proposed.[20]

The main idea of the present paper is to address the effect of a pulsating flow on the front propagation. Recently, Nolen and Xin[12] studied the effect of a time and space periodic flow on the front propagation velocity from a numerical and analytical point of view. They found that, in the limit of a weak flow velocity, the front velocity quadratically increases with the maximum flow velocity. Here, we experimentally focus on a more realistic flow where the mean space flow velocity is not zero. It corresponds to the one studied by Chatwin,[21] Smith,[22] and Watson[23] without reaction. They showed, by using a Taylor-like approach,[19] that in the tracer case, a pulsating flow results in an effective time dependent diffusion coefficient, the time average of which is larger than the molecular diffusion coefficient.[23] In the same spirit, we will focus on the time-averaged front velocity obtained in the mixing regime, in the presence of an oscillating flow, of period T. More precisely, we address the low frequency regime and accordingly discuss the relevant time scale, to which the time scale of the flow T has to be compared.

We study, experimentally and numerically, a third-order autocatalytic IAA reaction submitted to a pulsative flow. In Sec. I, we present the experimental setup and the measurements obtained in a Hele–Shaw (HS) cell by using various frequencies and amplitudes of oscillations. In Sec. II, we compare the experimental results with two-dimensional (2D) numerical simulations involving an oscillating Poiseuille flow. In Sec. III, we focus on the Taylor regime. First, we delineate the Taylor regime in the case of a stationary Poiseuille profile.[18,20] Then, we extend the results to the quasistatic regime of an oscillating flow.

EXPERIMENTAL SETUP AND DATA

We use the third-order autocatalytic IAA reaction. The reaction front is detected with starch, which leads to a dark blue signature of the transient iodine as the reaction occurs.[1,6,13] In the absence of flow, a reaction front travels similar to a solitary wave, with a constant velocity $V_\chi^{\exp}\sim 20\ \mu$m/s and with a stationary concentration profile of width $l_\chi^{\exp}\sim 100\ \mu$m in agreement with the theoretical one (Eq. (2)). We study the front propagation in a HS cell of

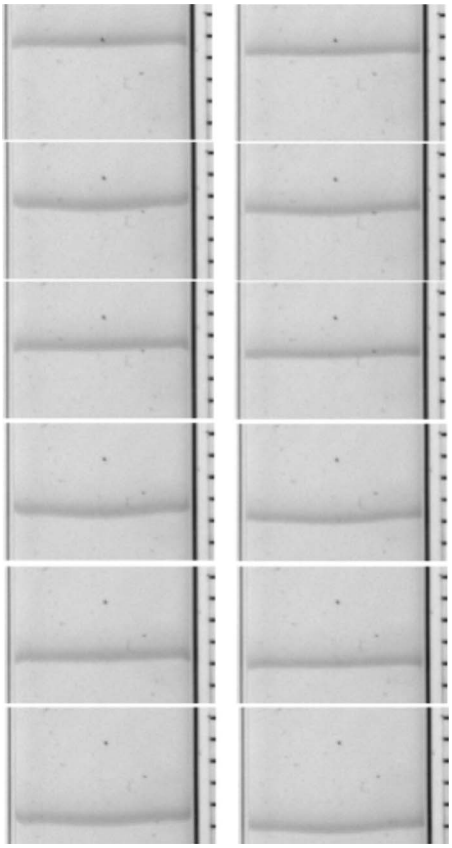

FIG. 2. Time evolution of a chemical front (in y-z plane) in a pulsative flow field of period $T=50$ s and velocity amplitude $U_M=69.1\ \mu$m/s. Time increases from left to right and from top to bottom. Two images are separated by $T/4$ time intervals. The distance between two dashes is 1 mm.

cross section $b\times h=0.4\times 8$ mm^2 (along the x and y directions, respectively). The unidirectional (along the z direction) oscillating flow is imposed at the bottom of a vertical HS cell, from a reservoir filled with unreacted species. The reservoir is closed with a thin elastic membrane, which is deformed by a rigid rod fixed at the center of a loudspeaker. Consequently, a displacement of a given volume of liquid in the reservoir induces a displacement of the same volume of liquid in the HS cell. The y-z plane of the HS cell is enlightened from behind and recorded with a charge coupled device camera. The amplitude A and the pulsation $\omega=2\pi/T$ of the oscillating flow are imposed by the controlled sine tension applied to the loudspeaker and measured *in situ* from the recorded displacement of the air/liquid interface at the top of the partially filled HS cell. This displacement obeys the expected $A\sin(\omega t)$ time dependence. Due to the constraint of our device, the imposed amplitude A and frequency f of the flow displacement are in the ranges of $A\in[0.07\text{ mm},1.7\text{ mm}]$ and $f\in[0.01\text{ Hz},0.2\text{ Hz}]$. The oscillating flow field in the HS cell is of the form $f(x,y,t)$. The shape of the velocity profile depends on the viscous penetration length $l_\nu=\sqrt{\nu/\omega}$.[24] If l_ν is large compared to the cell thickness b (low frequency), the flow variations are slow enough for the steady state to be established. The resulting "oscillating stationary" velocity profile is parabolic in the gap and flat along the width h of the cell except in the vicin-

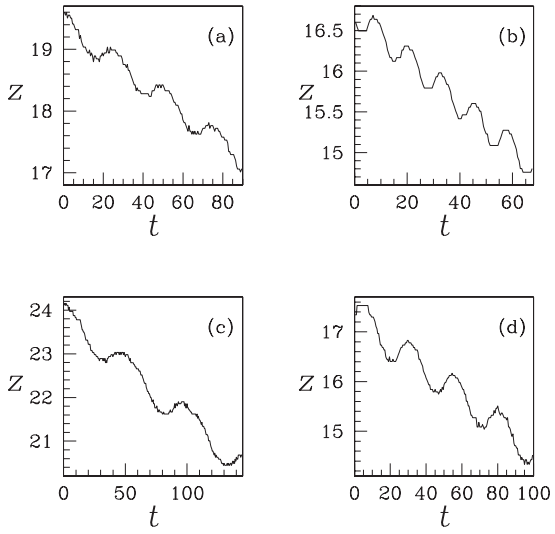

FIG. 3. Time evolution of the front position, $z(t)$ (z in mm, t in s), for different values of the periods and velocity amplitudes corresponding to (T, U_M) (T in s and U_M in μm/s). (a) (25, 70.4), (b) (50, 69.1), (c) (12.5, 140.7), and (d) (25, 138.2).

ity of the side walls, in a layer of thickness b.[25] Figure 1 is a sketch of such an effect.

Conversely, for $l_\nu \ll b$ (high frequency), the fluid has not enough time to feel the effects of the solid boundaries and the velocity profile is flat over the whole cross section $b \times h$, except in the vicinity of the walls, in a layer of thickness l_ν. For our dilute aqueous solutions of viscosity $\nu \approx 10^{-6}$ m^2 s^{-1} and in our frequency range, the penetration length l_ν, which lies between 0.8 and 4 mm, is larger than the cell thickness $b=0.4$ mm. Hence, the "stationary velocity profile" is expected to be instantaneously reached. It is parabolic, Poiseuille-like across the gap b, and almost flat along the y direction (except in a layer of thickness b close to the sides of the cell). In our experiments, the flow velocity profile can then be approximated by

$$U(x,t) = U_M\left(1 - \frac{4x^2}{b^2}\right)\cos(\omega t), \tag{3}$$

where $U_M = A\omega$ is the velocity amplitude in the middle of the gap (at $x=0$). Figure 2 displays snapshots (in y-z plane) of a typical experiment.

We do observe a front slightly deformed, which propagates up and down (oscillating), with a downward averaged displacement from the burnt product of the reaction to the fresh reactant. From such a frame sequence, the front is tracked and its location is plotted as a function of time. Figure 3 shows the front position $z(t)$ so obtained, its oscillation at roughly the imposed frequency, and an overall drift of the front for various amplitudes and periods of the flow.

The measurement of this drift in time leads to the time-averaged front velocity $\langle V_f^{\exp}\rangle$. Figure 4 displays $\langle V_f^{\exp}\rangle$, normalized by $V_\chi^{\exp}$, versus the flow velocity amplitude U_M, also normalized by $V_\chi^{\exp}$. The increase in $\langle V_f^{\exp}\rangle$ with U_M is almost linear, with a slope slightly larger than 0.1. This demonstrates that the propagation velocity of a reaction front can be enhanced by a null in average, laminar flow. Moreover, as

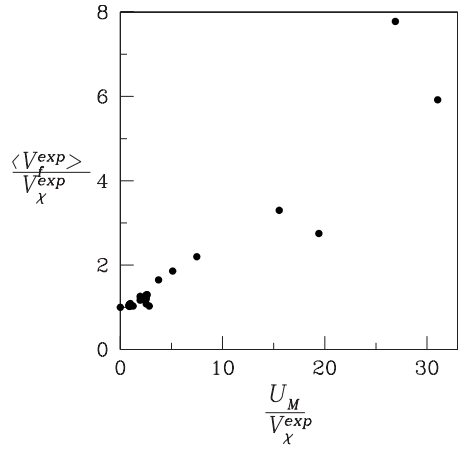

FIG. 4. Normalized drift velocity of the chemical front $\langle V_f^{\exp}\rangle / V_\chi^{\exp}$ vs the normalized flow velocity amplitude $U_M / V_\chi^{\exp}$.

the mean advection in this time-periodic flow is zero, this effect clearly comes from some nonlinear interplay. It might be attributed to the enhancement of the mixing by the flow.

As mentioned above, it is seen from the instantaneous displacement of the front that the front velocity oscillates at the frequency of the flow. We also noticed from our observation of the experimental movies that the width of the colored front $L(t)$ was likely to oscillate at a frequency twice that of the excitation, which, unfortunately, is not obvious on the static pictures (such as Fig. 2). To confirm this empirical observation, we measured the width $L(t)$ of the dark blue ribbon. As this ribbon corresponds to the presence of the transient iodine, $L(t)$ is an indirect measure of the chemical front width, but it gives, however, the right time behavior. A classical Fourier analysis of $L(t)$ was tried but due to the large amount of noise, it did not provide any reliable frequency dependence. Therefore, we used the more sensitive micro-Doppler method (see Refs. 26 and 27, and the references therein), which analyzes the instantaneous signal frequency. The so-obtained oscillation frequencies f' of the width $L(t)$ versus the imposed ones f are displayed in Fig. 5.

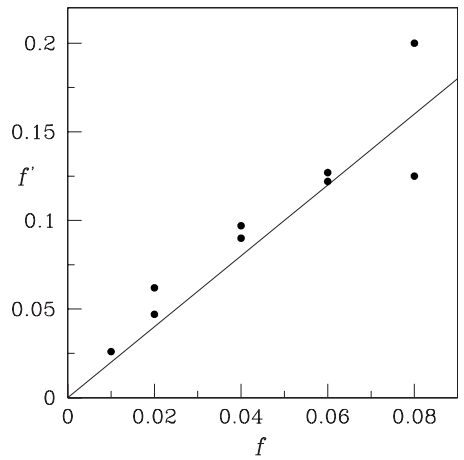

FIG. 5. Experimental oscillation frequency f' of the front width vs the imposed oscillation frequency f of the flow (in Hz). The straight line is $f'=2f$.

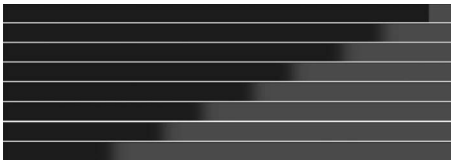

FIG. 6. 2D numerical simulation of the front displacement (in the gap of the cell, x-z plane), which is obtained with an imposed flow of period and amplitude, $T=10^6$ and $U_M=2\pi\times10^{-5}$. The product of the reaction is in gray and the reactant is in dark. From top to bottom, time increases by 2×10^5 time steps. The lattice dimensions are 40×4000. Note that the aspect ratio of the pictures is not 1.

Their collapse onto the straight line $f'=2f$ demonstrates that the front width oscillates at twice the frequency of the flow. We note that this feature could support the description of the front thickness in the framework of an effective diffusion coefficient D, since the latter is expected to be insensitive to the flow direction and to depend only on the flow amplitude, which follows $D\propto U^2$ (which here oscillates at $2f$).[8] We note also that this feature might be attributed to the deformation (in the gap) of the front by the flow, which could stretch the front during the displacement either forwards or backwards. To have further insight into the instantaneous features of the propagating front, we used numerical simulations, which give access to the behavior in the gap of the cell.

COMPARISON WITH 2D NUMERICAL SIMULATIONS

Assuming a third-order autocatalytic reaction kinetics for the IAA reaction[1,6,13] and a unidirectional flow $U(x,y,t)$ in the z direction, the ADR equation (1) reads

$$\frac{\partial C}{\partial t}+U\frac{\partial C}{\partial z}=D_m\left(\frac{\partial^2 C}{\partial x^2}+\frac{\partial^2 C}{\partial z^2}\right)+\alpha C^2(1-C), \tag{4}$$

where C is the concentration of the (autocatalytic) reactant iodide, which is normalized by the initial concentration of iodate, D_m is the molecular diffusion coefficient, and α is the kinetic rate coefficient of the reaction. The solution of Eq. (4) was generated by using a lattice Bhatnagar–Gross–Krook (BGK) method. This method is described in detail in Ref. 28 and has already been used in similar contexts.[17,25,29,30] Equation (4) was solved in two dimensions (in the gap of the cell, x-z plane) by using the analytical Poiseuille velocity field given by Eq. (3), which holds in the low frequency regime, $T\gg\tau_\nu=b^2/\nu$.

To compare the results of the numerical simulations with the experiments, we used the same nondimensional quantities, namely, $U_M/V_\chi^{\exp}$ and $b/l_\chi^{\exp}=4$. The simulations were performed on a lattice of length N_z which ranges between 2000 and 6000 nodes, and of constant width $N_x=40$ nodes during 2×10^5 to 4×10^6 iterations. The above experimental value of $b/l_\chi^{\exp}$ gives a numerical chemical length $l_\chi=N_x l_\chi^{\exp}/b=10=\sqrt{2D_m/\alpha}$. We chose $D_m=5\times10^{-3}$ and $\alpha=10^{-1}$, which set the front velocity to $V_\chi=\sqrt{\alpha D_m/2}=5\times10^{-4}$. The varying parameters in the simulations are the velocity amplitude U_M and the period T of the imposed oscillating flow.

A typical time sequence of a numerical simulation is displayed in Fig. 6. It can be seen that the front oscillates and travels from the burnt product to the fresh reactant. The mean concentration profiles were obtained by averaging across the lattice width and analyzed along the same line as in the experiments. Figure 7 shows the time evolution of the displacement of the isoconcentration $\bar{C}=0.5$, which is measured in 2D simulations and in experiments: The agreement between the two supports the contention that in our frequency range, the dynamics of the front is governed only by the variations of the velocity field in the gap ($b=0.4$ mm), and that the (large) transverse extent of the plane of the experimental cells ($h=8$ mm) plays no role.

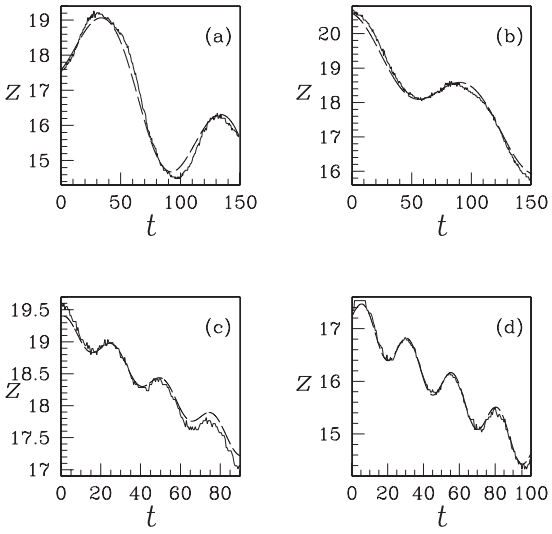

FIG. 7. Time evolution of the front position, $z(t)$ (z in mm, t in s). –: Experimental data and – –: numerical simulations. The experimental values (T, U_M) (T in s and U_M in μm/s) are (a) (1.12, 100, 70.4), (b) (0.55, 100, 34.6), (c) (0.14, 25, 35.2), and (d) (0.14, 12.5, 70.4).

STUDY OF THE LOW FREQUENCY TAYLOR'S REGIME

By taking advantage of the flexibility of the numerical simulations, we have investigated the low frequency mixing regime and compared it to the corresponding regime that one can extrapolate from the stationary flow cases.[16–18,20] To address Taylor's mixing regime in slowly oscillating flows, we will recall first the main expressions obtained for stationary flows in the frame of Taylor's description and study their range of validity in the case of a Poiseuille flow.

We showed in Ref. 18 that, in the asymptotic mixing regime, the extension l_f of the transverse-averaged concentration $\bar{C}$ (defined by $l_f^2=(3/\pi^2)\int_{-\infty}^{+\infty}z^2(d\bar{C}/dz)dz$) could be expressed as $l_f=\sqrt{2D_{\text{eff}}/\alpha}$, where D_{eff} is the effective Taylor diffusion coefficient, which reads, for the Poiseuille flow in the gap of a HS cell, as

$$\frac{D_{\text{eff}}}{D_m}=1+\frac{1}{210}\left(\frac{\bar{U}b}{D_m}\right)^2=1+\frac{2}{945}\left(\frac{b}{l_\chi}\right)^2\left(\frac{U_M}{V_\chi}\right)^2, \tag{5}$$

with $\bar{U}$ and $U_M=3\bar{U}/2$ as the average and the maximum of the fluid velocity, respectively. In this regime, the front velocity,

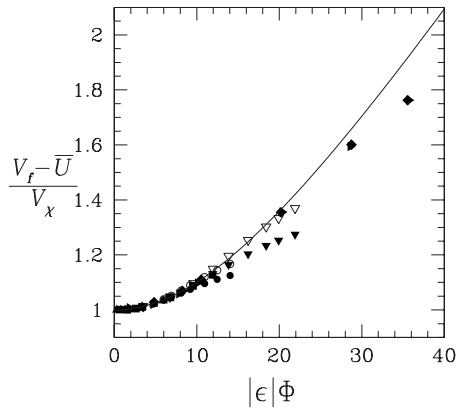

FIG. 8. Normalized relative front velocity, $(V_f-\bar{U})/V_\chi$, vs $|\epsilon|\phi$, where $\epsilon=U_M/V_\chi$ and $\phi=b/l_\chi$ are the Poiseuille flow and lattice parameters. The symbols pertain to different values of (ϵ,l_χ). ●: (0.75, 15.8), ▲: (0.75, 31.6), ▼: (1.5, 15.8), ■: (1.5, 31.6), ◆: (4.5, 15.8), and ▶: (4.5, 31.6). The open symbols correspond to negative values of ϵ. The line is the theoretical prediction of Eq. (7).

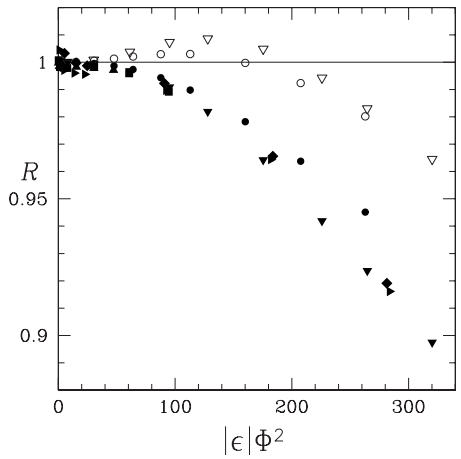

FIG. 9. Ratio of the normalized relative front velocity to the mixing regime contribution, $R=(V_f-\bar{U})/V_\chi\sqrt{1+(2/945)(\epsilon\phi)^2}$, vs $|\epsilon|\phi^2$. The symbols are the same as in Fig. 8. The straight line is the theoretical prediction of Eq. (7).

$$V_f=\bar{U}+\sqrt{\alpha D_{\text{eff}}/2}, \tag{6}$$

is the sum of the advection by the mean flow and a relative velocity $\sqrt{\alpha D_{\text{eff}}/2}>V_\chi$, which accounts for the enhancement of the dispersion caused by a nonuniform flow. We note that the normalized relative front velocity depends on the normalized flow velocity $\epsilon=U_M/V_\chi$ and on the ratio $\phi=b/l_\chi$, as follows:

$$\frac{V_f-\bar{U}}{V_\chi}=\sqrt{\frac{D_{\text{eff}}}{D_m}}=\sqrt{1+\frac{2}{945}(\epsilon\phi)^2}. \tag{7}$$

We first tested the validity of the above prediction with 2D numerical simulations of the autocatalytic chemical reaction in a Poiseuille flow. The molecular diffusion coefficient was set to $D_m=5\times10^{-2}$ and two series of simulations were performed, with the reaction rates $\alpha=10^{-3}$ and 4×10^{-3}. This provided front widths and velocities $(l_\chi,V_\chi)=(31.6,0.0016)$ and (15.8, 0.0032). The mean flow rate $\bar{U}$ and the width b of the lattice, were subsequently varied, to obtain the following values $|\epsilon|=U_M/V_\chi=0.75$, 1.5, and 4.5 and a ratio $\phi=b/l_\chi$ ranging between 0.4 and 15. Figure 8 displays the normalized relative front velocity as a function of $|\epsilon|\phi$. At low values of $|\epsilon|\phi$, the data collapse onto the theoretical prediction given by Eq. (7) but a discrepancy is observed when $|\epsilon|\phi$ is increased. We note that the departure from our model occurs at $|\epsilon|\phi$ values, which are different for each set of data.

The departure from Taylor's mixing regime is expected to occur when the typical diffusion time across the lattice width, $\tau_D=b^2/D_m$, is not any more small compared to the typical advection time by the flow, along the front width, $\tau_{\text{ad}}=l_\chi/\bar{U}$. This condition writes $\tau_D\geqslant\tau_{\text{ad}}$, or equivalently,

$$|\epsilon|\phi^2\geqslant 1. \tag{8}$$

This analysis suggests that the combined parameter $|\epsilon|\phi^2$ may be relevant to delineate Taylor's mixing regime of autocatalytic reaction fronts. Accordingly, we plotted in Fig. 9 the ratio R of the normalized relative front velocity to Taylor's mixing regime effect [right hand side of Eq. (7)] as a function of $|\epsilon|\phi^2$. Figure 9 shows that, whatever the values of $|\epsilon|$ or ϕ are, the data collapse onto Taylor's mixing regime prediction $R=1$, for values of $|\epsilon|\phi^2$ smaller than roughly 100, and deviate within 4% of the latter regime, for $|\epsilon|\phi^2\simeq200$. We note that in this range of small deviation from the prediction, the deviation has the opposite sign of ϵ: it is positive for adverse flows and negative for supportive flows. This is consistent with the contribution to the front velocity $D_m\mathcal{K}$ of the curvature $\mathcal{K}$ of a steady shape traveling front[17] in the eikonal regime. Indeed, the deformation by the flow of the isoconcentration curves leads to opposite curvatures in adverse or supportive flows.

It is of practical interest to note that Taylor's mixing regime prediction for the velocity of an autocatalytic reacting front in a stationary flow, which holds for values of the parameter $|\epsilon|\phi^2$ smaller than a few hundreds, will remain valid for large fluid velocities in small-scale devices (as in microfluidic systems).

We now turn to analyze the influence of an oscillating flow on the front velocity. Here, we are interested in the approach toward the asymptotic Taylor's mixing regime, which is extrapolated from the stationary flow case.

This extrapolation is obtained by replacing in the effective diffusion coefficient expression (5) the maximum velocity U_M by its instantaneous counterpart, $U_M\cos(\omega t)$. This leads to the following time-averaged relative front velocity:

$$\frac{\langle V_f-\bar{U}\rangle}{V_\chi}=\left\langle\sqrt{\frac{D_{\text{eff}}}{D_m}}\right\rangle=\left\langle\sqrt{1+\frac{2}{945}(\epsilon\phi)^2\cos^2(\omega t)}\right\rangle. \tag{9}$$

We note that for the sine flow of interest, the mean advection is null, $\langle\bar{U}\rangle=0$. Equation (9) gives then the normalized time-averaged front velocity $\langle V_f\rangle/V_\chi$. The latter is actually increased by the mixing of the flow $(\langle V_f\rangle/V_\chi>1)$, by an amount which depends on the product $\epsilon\phi$. Hence, the front velocity increase depends on the intensity of the flow (through $\epsilon=U_M/V_\chi$) but not on the flow period T. This last

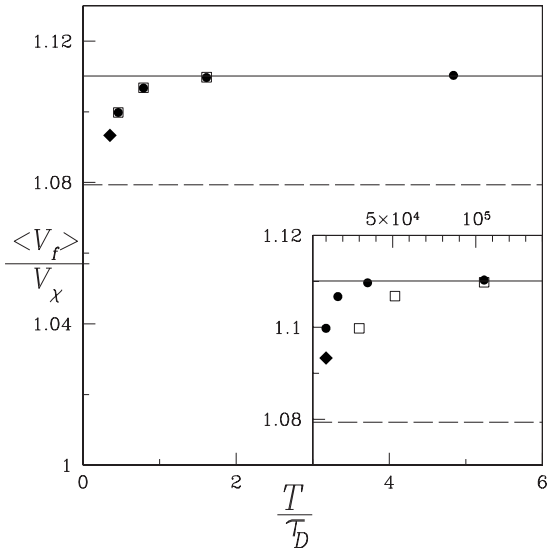

FIG. 10. Normalized time-averaged front velocity $\langle V_f \rangle / V_\chi$ versus the flow period T (inset) and versus the normalized flow period T/τ_D. The symbols correspond to different values of τ_D. ●: $\tau_D = 2.17 \times 10^4$, ◆: 2.84×10^4, and □: 6.50×10^4. The solid line corresponds to Taylor's mixing regime prediction, which is given by Eq. (9). The dashed line corresponds to analytical fit of Ref. 20.

feature results from the quasistatic conditions, under which the stationary case applies at each time: the variations are slow enough for both the stationary flow field and the stationary chemical front shape to be established. Quantitatively, the quasistatic conditions require the flow period T to be large compared to the typical diffusion time across the width τ_D and to the typical advection time along the front width τ_{ad}. We have tested the approach toward the quasistatic prediction, with numerical simulations performed at $b=19$, $\phi = b/l_\chi = 1$, and $\epsilon = U_M/V_\chi = 15$, which correspond to $\epsilon\phi = 15$ and $\epsilon\phi^2 = 15$. The flow period T was varied from $T = 10^4$ to 20×10^4, and the typical diffusion times were chosen equal to $\tau_D = 2.17 \times 10^4$, 2.84×10^4, or 6.50×10^4. The inset of Fig. 10 displays the normalized time-averaged front velocity, $\langle V_f \rangle / V_\chi$ as a function of the flow period T for different values of the typical diffusion time τ_D. The quasistatic prediction of Eq. (9) is displayed as a solid straight line in Fig. 10. It is seen that when T is large enough compared to τ_D, the front velocity reaches the asymptotic value of Taylor's mixing regime. On the other hand, the smaller the flow period is, the larger the deviation from that value is. It can also be noticed that the discrepancy between the numerical results and Taylor's limit increases with τ_D. This suggests to normalize T by the corresponding τ_D. Figure 10 shows the resulting superposition of the data obtained at different τ_D. For the particular values $\epsilon\phi = 15$ and $\epsilon\phi^2 = 15$ used in the present simulations, Taylor's mixing regime is reached as soon as $T \simeq 2\tau_D$. Also shown (dashed lines in Fig. 10) is the average, over the period T, of the analytical expression of Ref. 20, which is obtained by fitting the numerical simulation results of the ADR equation (1) under stationary conditions. We note that the latter analysis, which addressed a wide range of intermediate ϕ and finite ϵ,[20] slightly underestimates the asymptotic front velocity in the Taylor regime domain.

CONCLUSION

In this paper, we have analyzed the influence of a low frequency time-periodic flow on the propagation of a third-order autocatalytic reaction front in a HS cell. The numerical simulations, which are in reasonable agreement with the experiments, show that the front dynamics is controlled by the Poiseuille flow in the gap of the cell. We have checked that for a stationary Poiseuille flow, the front propagation can be described by using a Taylor approach when the product of the normalized flow velocity by the Thiele modulus $\epsilon\phi^2$ does not exceed some hundreds. This Taylor approach applies for periodic flows in a quasistatic regime, which has been shown to hold for flow periods T, which are lower than the characteristic diffusion time across the front width. Under these conditions, our Taylor mixing prediction is found to be in accordance with the front velocities measured in the simulations.

ACKNOWLEDGMENTS

We thank Dr. Céline Lévy-Leduc for fruitful discussions. This work was partly supported by IDRIS (Project No. 034052), CNES (No. 793/CNES/00/8368), ESA (No. AO-99-083), and MRT grants (for M. Leconte and N. Jarrige). All these sources of support are gratefully acknowledged.

[1] S. K. Scott, *Oscillations, Waves and Chaos in Chemical Kinetics* (Oxford University Press, Oxford, 1994).
[2] P. Clavin, "Dynamic behavior of premixed flame fronts in laminar and turbulent flows," Prog. Energy Combust. Sci. **11**, 1 (1985).
[3] R. A. Fisher, "The wave of advance of advantageous genes," Proc. Annu. Symp. Eugen. Soc. **7**, 355 (1937).
[4] A. N. Kolmogorov, I. G. Petrovskii, and N. S. Piskunov, "A study of the diffusion equation with increase in the quantity of matter, and its application to a biological problem," Moscow Univ. Bull. Math. **1**, 1 (1937).
[5] P. A. Epik and N. S. Shub, "Frontal progress of the oxidation reaction of arenite with iodate," Dokl. Akad. Nauk SSSR **100**, 503 (1955).
[6] A. Hanna, A. Saul, and K. Showalter, "Detailed studies of propagating fronts in iodate oxidation of arsenous acid," J. Am. Chem. Soc. **104**, 3838 (1982).
[7] Y. B. Zeldovitch and D. A. Franck-Kamenetskii, "A theory of thermal propagation of flame," Acta Physicochim. URSS **9**, 341 (1938).
[8] U. Ebert and W. van Saarloos, "Front propagation into unstable states: Universal algebraic convergence towards uniformly translating pulled fronts," Physica D **146**, 1 (2000).
[9] G. Papanicolaou and J. Xin, "Reaction-diffusion front speeds in periodically layered media," J. Stat. Phys. **63**, 915 (1991).
[10] B. Audoly, H. Berestycki, and Y. Pomeau, "Réaction-Diffusion en écoulement rapide," C. R. Acad. Sci., Ser. IIb: Mec., Phys., Chim., Astron. **328**, 255 (2000).
[11] M. Abel, A. Celani, D. Vergni, and A. Vulpiani, "Front propagation in laminar flows," Phys. Rev. E **64**, 046307 (2001).
[12] J. Nolen and J. Xin, "Reaction-diffusion front speeds in spatially-temporally periodic shear flows," Multiscale Model. Simul. **1**, 554 (2003).
[13] M. Böckmann and S. C. Müller, "Growth rate of the buoyancy-driven instability of an autocatalytic reaction front in a narrow cell," Phys. Rev. Lett. **85**, 2506 (2000).
[14] L. Szirovicza, I. Nagypál, and E. Boga, "An algorithm for the design of propagating acidity fronts," J. Am. Chem. Soc. **111**, 2842 (1989).
[15] D. Horváth and Á. Tóth, "Diffusion-driven front instabilities in the chlorite-tetrathionate reaction," J. Chem. Phys. **108**, 1447 (1998).
[16] B. F. Edwards, "Poiseuille advection of chemical reaction fronts," Phys. Rev. Lett. **89**, 104501 (2002).
[17] M. Leconte, J. Martin, N. Rakotomalala, and D. Salin, "Pattern of reaction

diffusion fronts in laminar flows," Phys. Rev. Lett. **90**, 128302 (2003).
[18]M. Leconte, J. Martin, N. Rakotomalala, D. Salin, and Y. C. Yortsos, "Mixing and reaction fronts in laminar flows," J. Chem. Phys. **120**, 7314 (2004).
[19]G. I. Taylor, "Dispersion of soluble matter in solvent flowing slowly through a tube," Proc. R. Soc. London, Ser. A **219**, 186 (1953); "Diffusion and mass transport in tubes," Proc. R. Soc. London, Ser. B **67**, 857 (1954).
[20]B. F. Edwards, "Propagation velocities of chemical reaction fronts advected by Poiseuille flow," Chaos **16**, 043106 (2006).
[21]P. C. Chatwin, "On the longitudinal dispersion of passive contaminant in oscillatory flows in tubes," J. Fluid Mech. **71**, 513 (1975).
[22]R. Smith, "Contaminant dispersion in oscillatory flows," J. Fluid Mech. **114**, 379 (1982).
[23]E. J. Watson, "Diffusion in oscillatory pipe flow," J. Fluid Mech. **133**, 233 (1983).
[24]L. Landau and E. Lifchitz, *Physique Théorique, Mécanique des Fluides* (Editions Mir, 1989).
[25]P. Gondret, N. Rakotomalala, M. Rabaud, D. Salin, and P. Watzky, "Viscous parallel flows in finite aspect ratio Hele-Shaw cell: Analytical and numerical results," Phys. Fluids **9**, 1841 (1997).
[26]I. Renhorn, C. Karlsson, D. Letalick, M. Millnert, and R. Rutgers, "Coherent laser radar for vibrometry: Robust design and adaptative signal processing," Proc. SPIE **2472**, 23 (1995).
[27]M. Lavielle and C. Lévy-Leduc, "Semiparametric estimation of the frequency of unknown periodic functions: Application to laser vibrometry signals," IEEE Trans. Signal Process. **53**, 2306 (2005).
[28]E. G. Flekkoy, "Lattice Bhatnagar-Gross-Krook models for miscible fluids," Phys. Rev. E **47**, 6 (1993).
[29]J. Martin, N. Rakotomalala, D. Salin, and M. Böckmann, "Buoyancy-driven instability of an autocatalytic reaction front in a Hele-Shaw cell," Phys. Rev. E **65**, 051605 (2002).
[30]N. Rakotomalala, D. Salin, and P. Watzky, "Miscible displacement between two parallel plates: BGK lattice gas simulations," J. Fluid Mech. **338**, 277 (1997).